energy&fuels

Article

pubs.acs.org/EF

Estimation of the SARA Composition of Crude Oils from Bubblepoint Pressure Data

D. Reyes-Gonzalez,[†] E. Ramirez-Jaramillo,[‡] O. Manero,[†] C. Lira-Galeana,*[,‡] and J. M. del Rio*[,‡]

[†]National University of Mexico, Ciudad Universitaria, Avenida Universidad 3000, Mexico City 04510, Mexico

[‡]Mexican Institute of Petroleum, Eje Central Lazaro Cardenas 152, Col. San Bartolo Atepehuacan, Mexico City 07730, Mexico

Supporting Information

ABSTRACT: A statistical correlation to provide reasonable estimates of crude oils SARA compositions (saturates, aromatics, resins, asphaltenes) from bubblepoint pressure and light-ends compositional data is presented. In developing the correlation, we collected experimental SARA compositions of 341 crude oils of different origin. The most-probable SARA compositions are then obtained by seeking the maximum probability according to its oil type, in line with the measured values of bubblepoint pressures. Results show that the proposed method is simple and provides reasonable values of SARA compositions of an oil in cases in which only the light-ends compositions and a few bubblepoint pressures are available.

INTRODUCTION

Reservoir fluid property variations with time during the production of oil cause multiple-phase and complex flow phenomena such as asphaltene deposition and wells plugging,[1] with high-cost impact in the economy of oil production.[2] Proper estimation of such variations is important for process design and production optimization.

Bubblepoint pressures, i.e., the pressures at which gas liberates from an oil, are among the various changing properties of a fluid that critically affect the efficiency of oil production. For instance, the inflow performance analysis of a well depends on the location and extent of the oils bubblepoint pressure, and so does the whole productivity behavior of a given facility. Bubblepoint pressures are important parts of the oils *PVT* study. SARA analyses provide further compositional information on the resin/asphaltene content of a producing fluid. For a flow-assurance study, of a given production asset, the SARA separations require extensive time and laboratory resources, and reproducibility issues have been a constant challenge.[3−5] To avoid this difficulty, a few calculation approaches for estimating the SARA composition of asphaltenic fluids have been reported in open literature.

Fahim[4,5] proposed two equations for calculating bubblepoint pressures of a number of Iranian live oils of asphaltenic nature. Fahim used laboratory data of various oils with different amounts of asphaltenes. His proposed expressions, which contain 15−17 model parameters, are functions of system temperature, crude oil composition, molecular weight, and the API gravity of the heptanes-plus fraction. When compared to the experimental bubblepoints from which the correlations were developed, this author's approach showed good agreement with the experimental data.

More recently, del Rio et al.[3] developed two general correlations for calculating bubblepoint and upper onset of asphaltene precipitation pressures for reservoir fluids, from an experimental database of multiple APEs and SARA compositions of live reservoir fluids. Their equations require, in one version, only the light-end composition of a fluid for accurate predictions. In a second version of the correlations, a single onset-of-asphaltene precipitation pressure point in pressure/temperature coordinates suffices to provide accurate APE and bubblepoint pressure predictions in wide temperature intervals.

Here, based on the statistical distribution of a broader database of experimental APE and light-end compositions of reservoir fluids, we have solved the del Rio et al.[3] inverse problem; i.e., from a given set of experimental bubblepoint pressure and light-end compositions (usually available for most reservoir fluids), we get the statistically most-probable SARA compositions, and the bubblepoint pressures of any reservoir fluid. In performing this process, however, we found that the additional multidimensionalities (arising from this new ill-posed problem) can be solved by a simple statistical and physically sound method. We first present the statistical basis of the proposed method and the step-by-step calculation results for a sample oil. The experimental and calculated results for 10 reservoir fluids of different origin are finally presented and discussed.

METHOD

In a previous work, del Rio et al.[3] plotted the bubblepoint pressure (P^{bp}) as a function of temperature (T) for a series of Mexican crude oils. For the range of temperatures studied, it was found that a correlation of $P^{bp}(T)$ can be described by a family of parallel straight lines, where, for each crude oil,

$$P^{bp} = f^{bp}(C^{bp}) + B^{bp} \quad (1)$$

where B^{bp} is a constant independent of the crude oil and $f^{bp}(C^{bp})$ is an independent term of the straight line. In the study by del Rio et al.,[3] it was proposed that $f^{bp}(C^{bp})$ depends on composition of the oil in the following form:

Received: March 15, 2016
Revised: July 25, 2016
Published: August 19, 2016

DOI: 10.1021/acs.energyfuels.6b00614
Energy Fuels 2016, 30, 6913−6922

Table 1. Crude Oil Classification by Their Geographical Sources in the Database

crude oil origin	no. of oils in the database
Africa	8
Asia (China, India, Iran)	27
Europe (Italy, Norway, Finland, Russia, Turquey)	24
North America (Alaska, Canada, USA, Mexico)	119
Central America	3
South America (Venezuela, Colombia, Brazil, Trinidad and Tobago)	75
others	85
total	341

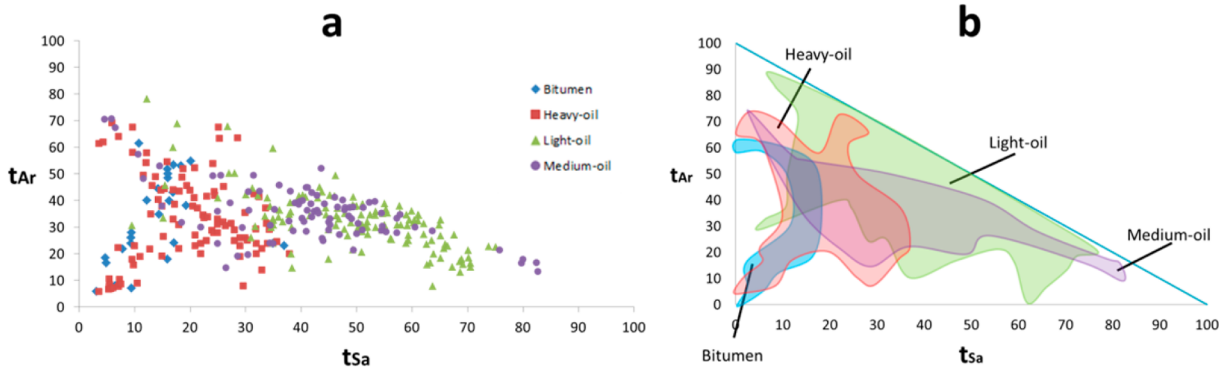

Figure 1. (a) Aromatic (t_{Ar})/saturate (t_{Sa}) composition distribution from 341 SARA data sets taken from the literature. Different symbols indicate different types of oil. (b) Bounded distributions for oil types of panel a.

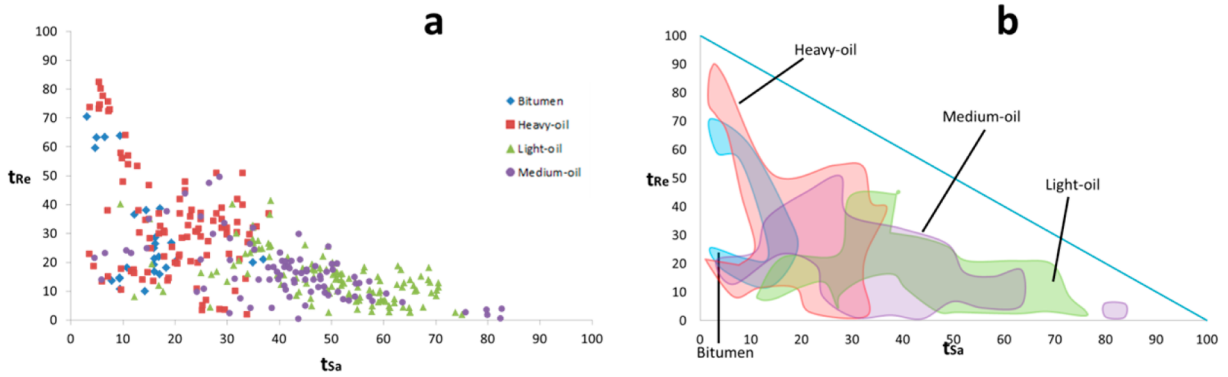

Figure 2. (a) Resin (t_{Re})/saturate (t_{Sa}) composition distribution from 341 SARA data sets taken from the literature. Different symbols indicate different types of oil. (b) Bounded distributions for oil types of panel a.

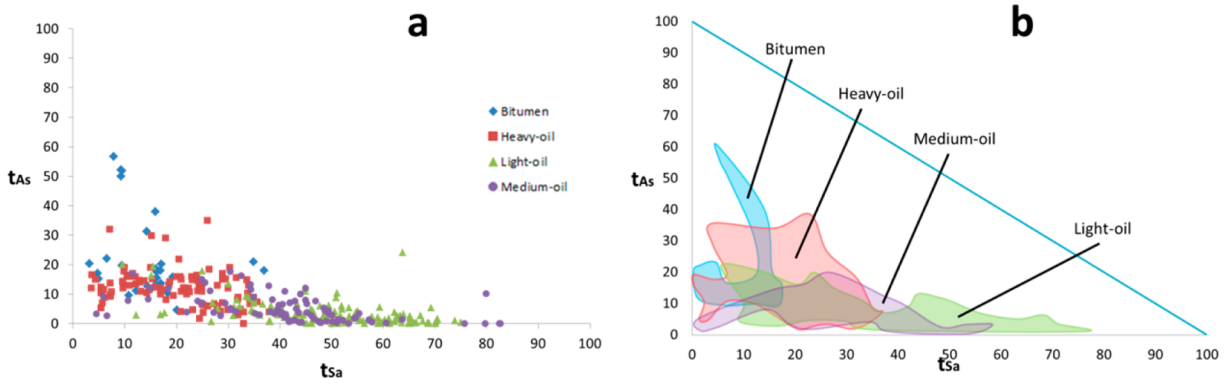

Figure 3. (a) Asphaltene (t_{As})/saturate (t_{Sa}) composition distribution from 341 SARA data sets taken from the literature. Different symbols indicate different types of oil. (b) Bounded distributions for oil types of panel a.

DOI: 10.1021/acs.energyfuels.6b00614
Energy Fuels 2016, 30, 6913−6922

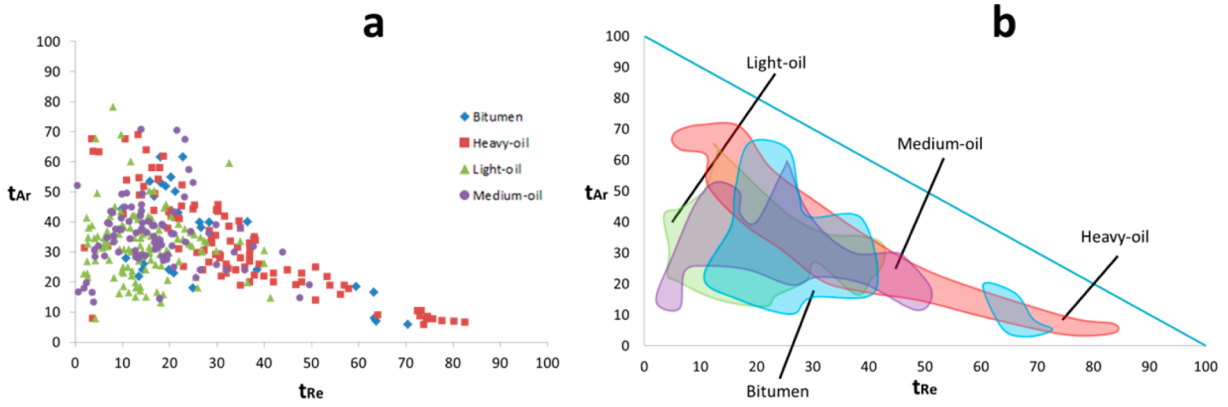

Figure 4. (a) Aromatic (t_{Ar})/resin (t_{Re}) composition distribution from 341 SARA data sets taken from the literature. Different symbols indicate different types of oil. (b) Bounded distributions for oil types of panel a.

$$f^{bp}(C^{bp}) = f_{H_2S}x_{H_2S} + f_{N_2}x_{N_2} + f_{CO_2}x_{CO_2} + f_{Sa}t_{Sa} + f_{Ar}t_{Ar} + f_{Re}t_{Re} + f_{As}t_{As} \quad (2)$$

where x_{H_2S}, x_{N_2}, and x_{CO_2} are the molar fractions of H_2S, N_2, and CO_2; t_{Sa}, t_{Ar}, t_{Re}, and t_{As} are the values of the SARA compositions in weight percent (wt %); and f_{H_2S}, f_{N_2}, f_{CO_2}, f_{Sa}, f_{Ar}, f_{Re}, and f_{As} are constants. The procedure to calculate all constant terms in eqs 1 and 2 is the following. All P^{bp} data as a function of temperature were fitted to a family of straight lines using a least-squares method. In this way, B^{bp} in eq 1, which is independent of the crude oil, was obtained. Additionally, a value of the independent term $f^{bp}(C^{bp})$ in eq 1 was obtained for each crude oil. The values of the coefficients f_{H_2S}, f_{N_2}, f_{CO_2}, f_{Sa}, f_{Ar}, f_{Re}, and f_{As} were calculated by fitting $f^{bp}(C^{bp})$ and composition data (x_{H_2S}, x_{N_2}, x_{CO_2}, t_{Sa}, t_{Ar}, t_{Re}, and t_{As}) from a set of 10 crude oils by a multivariable linear fit using eq 2. In this work, we address the inverse problem, i.e., for given values of the bubblepoint pressure as a function of temperature; we provide values of the most-probable SARA compositions for an asphaltenic oil, using a statistically coherent procedure.

To begin, let the probability density of an oil with a set of SARA compositions t_{Sa}, t_{Ar}, t_{Re}, and t_{As} be denoted as W; i.e.,

$$W = W(t_{Sa}, t_{Ar}, t_{Re}, t_{As}) \quad (3)$$

In practice, W can be obtained from a histogram of experimental SARA compositions. In this work, we have collected SARA compositions of 341 asphaltenic oils from different sources. Table 1 shows some features of our database. The set includes SARA analyses reported in 108 public papers found in open and private literature.[3,7−116] [An Excel-based data file containing SARA compositions, crude oil type, geographic region of origin, and bibliographic references for the whole set of 341 crude oils is available as Supporting Information.].

Figures 1−4 show the full set of experimental SARA compositions of these oils. From these figures it can be seen that SARA compositions distribute in regions according to the type of oil (light-oil, medium-oil, heavy-oil, and bitumen). It is interesting to note that the regions of light-oil, medium-oil, and heavy-oil get overlapped in some parts. Mathematically, this means that a same set SARA composition (t_{Sa}, t_{Ar}, t_{Re}, t_{As}) can, in principle, satisfy different types of oils. This condition prevents that a simple direct solution to this ill-posed mathematical problem, could be used. Toward developing a physically coherent solution procedure, we have considered different probability densities for each type of oil.

Instead of looking for the SARA compositions that give a maximum to the probability density function, W, we rather seek for the SARA composition which provides the maximum probability of the separated density functions, in line with values of the bubblepoint pressure. This formulation is illustrated as follows.

Let us consider a probability density of the form

$$W = W(x, y) \quad (4)$$

where x and y are two random variables whose plot is given in Figure 5a. If we would be interested in the most-probable point (x,y), we

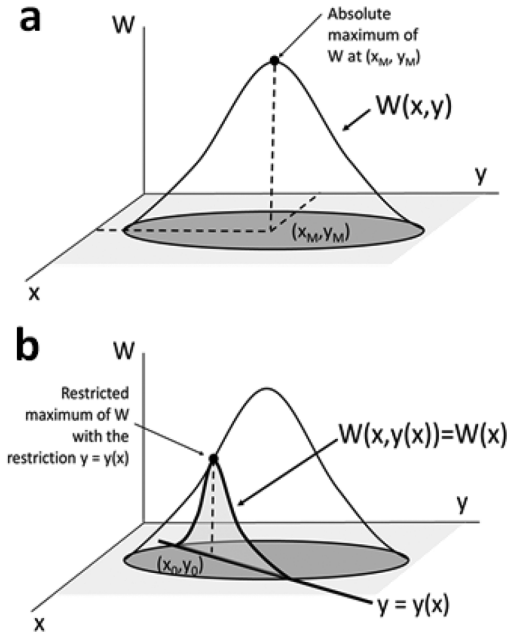

Figure 5. (a) Sketch of $W = W(x,y)$ reaching an absolute maximum at (x_M, y_M). (b) Example of the restriction $y = y(x)$, the restricted function $W(x)$, and the restricted maximum (x_0, y_0).

would then calculate the maximum of $W(x,y)$, denoted here as (x_M, y_M). But we are rather interested in a point (x,y) with the highest probability as possible, while being compatible with a certain closure characteristic. This characteristic can be written mathematically as

$$f(x, y) = \text{constant} \quad (5)$$

or, using the implicit form, as

$$y = y(x) \quad (6)$$

As example, Figure 5b shows the simple case:

$$y = ax + b \quad (7)$$

where a and b are constants. The values of W on this straight line are expressed as

DOI: 10.1021/acs.energyfuels.6b00614
Energy Fuels 2016, 30, 6913−6922

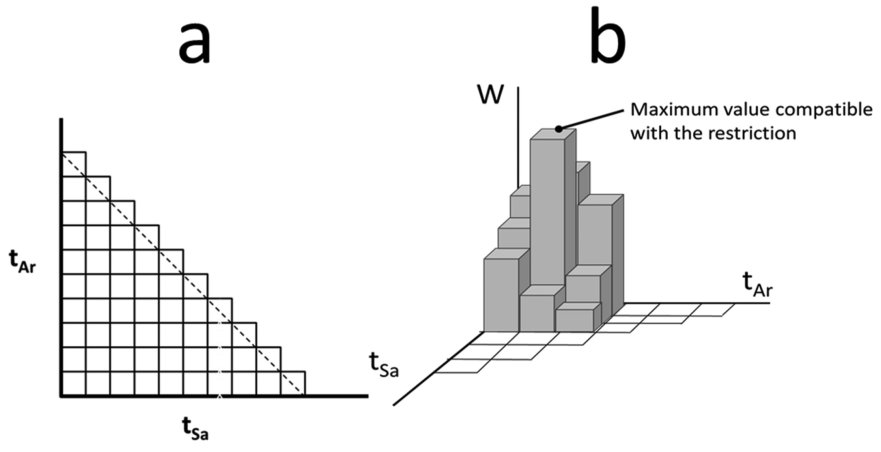

Figure 6. (a) Example of the mesh in a plot of t_{Ar} versus t_{Sa}. (b) Sample calculation of the function $W(t_{Sa},t_{Ar})$ in each cell of the mesh shown in panel a.

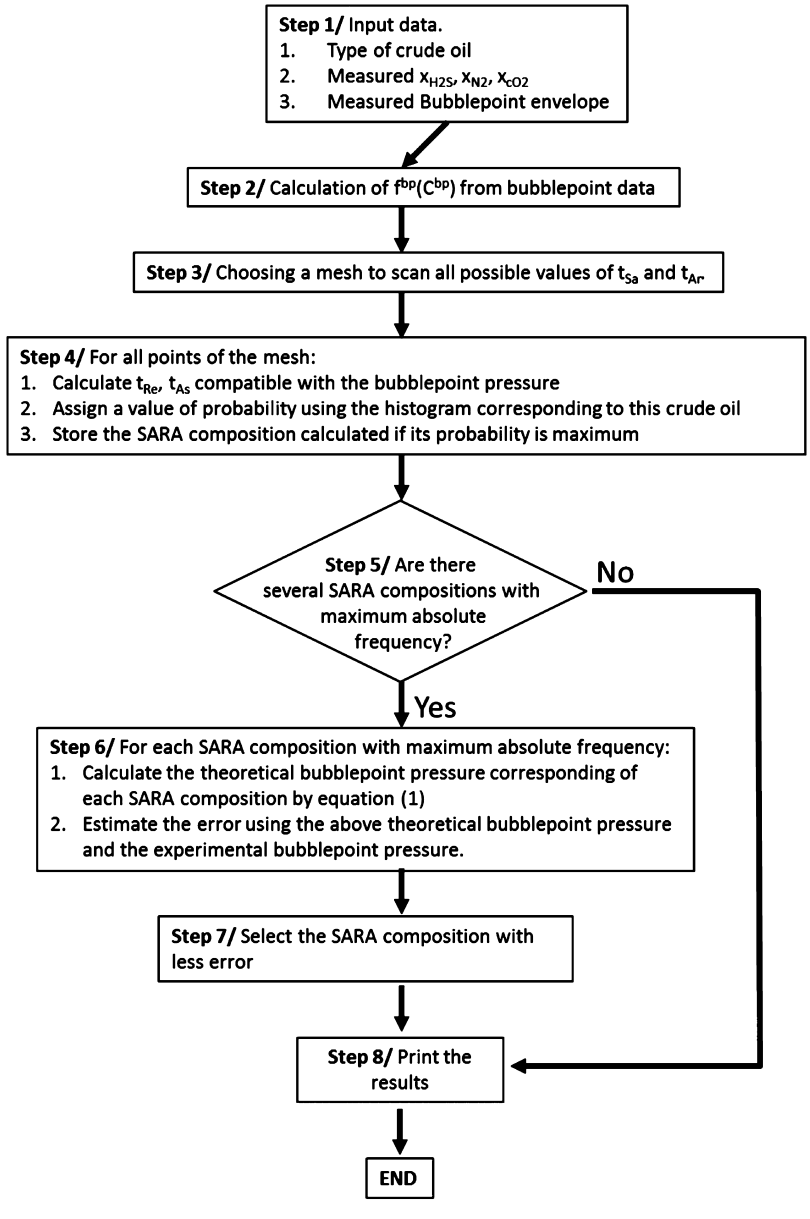

Figure 7. Calculation steps of the proposed method.

DOI: 10.1021/acs.energyfuels.6b00614
Energy Fuels 2016, 30, 6913−6922

$$W(x, y(x)) = W(x) \tag{8}$$

Equation 8 gives the values of W only for the points that fulfill the restraint given by eq 7. For this reason, at (x_0,y_0) (see Figure 5b) we reach the highest probability as possible, in accordance with the desired restraint.

If we would get the analytical functions of $W = W(x,y)$ and $y = y(x)$, we could use standard numerical methods of high accuracy to calculate the point (x_0,y_0). Here, those functions are not analytically available, because we have only data tables of the functions $W = W(x,y)$ and $y = y(x)$. In this case, a simple method to calculate the restricted maximum is to pick up a mesh on the curve $y = y(x)$ in order to calculate W in each point of the mesh and then take the point with the maximum value.

In our case, the functional restrictions for the SARA compositions were chosen in the following way. First, all SARA compositions are non-negative:

$$t_{Sa}, t_{Ar}, t_{Re}, t_{As} \geq 0 \tag{9}$$

Second, the four SARA compositions must add up to 100 wt %:

$$t_{Sa} + t_{Ar} + t_{Re} + t_{As} = 100 \tag{10}$$

The third consideration is that the SARA compositions must be consistent with the behavior of the bubblepoint pressure envelope considered. This condition can be obtained by combining eqs 1 and 2 as

$$f_{Sa}t_{Sa} + f_{Ar}t_{Ar} + f_{Re}t_{Re} + f_{As}t_{As} = P^{bp} - B^{bp}T - f_{H_2S}x_{H_2S} - f_{N_2}x_{N_2} - f_{CO_2}x_{CO_2} \tag{11}$$

The set of eqs 9−11 are equations similar to eq 5. The analogous equations to eq 7 can be obtained by combining eqs 10 and 11 as

$$t_{Re}(t_{Sa}, t_{Ar}) = 100 - \frac{K}{f_{As} - f_{Re}} - \left[1 + \frac{f_{Sa}}{f_{As} - f_{Re}}\right]t_{Sa} - \left[1 + \frac{f_{Ar}}{f_{As} - f_{Re}}\right]t_{Ar} \tag{12}$$

$$t_{As}(t_{Sa}, t_{Ar}) = \frac{K}{f_{As} - f_{Re}} - \frac{f_{Sa}}{f_{As} - f_{Re}}t_{Sa} - \frac{f_{Ar}}{f_{As} - f_{Re}}t_{Ar} \tag{13}$$

where K can be obtained from

$$K = P^{bp} - B^{bp}T - f_{H_2S}x_{H_2S} - f_{N_2}x_{N_2} - f_{CO_2}x_{CO_2} \tag{14}$$

Equations 12 and 13 give the relation between (t_{Sa}, t_{Ar}) and (t_{Re}, t_{As}) when the bubblepoint is considered. In this way eq 3 is then cast to

$$W(t_{Sa}, t_{Ar}, t_{Re}(t_{Sa}, t_{Ar}), t_{As}(t_{Sa}, t_{Ar})) = W(t_{Sa}, t_{Ar}) \tag{15}$$

Equation 15 provides the probability of finding a particular SARA composition in line with the bubblepoint. In this way, its maximum will give us the most-probable SARA composition.

In our case, a bidimensional mesh, such as the one shown in Figure 6, can be used, and the values of W can be calculated from the center points of each cell of the mesh using eq 15 (see Figure 6a). To close this problem, the SARA composition which gives the maximum value in W gives the most-probable SARA composition set, in line with the bubblepoint pressure.

RESULTS AND DISCUSSION

Figures 1−4 show respectively the aromatic SARA compositions versus the saturate SARA compositions; the resin SARA compositions versus the saturate SARA compositions; the asphaltene SARA compositions versus the saturate SARA compositions, and the aromatic SARA compositions versus resin SARA compositions. In all cases, the data were taken from our database,[7−116] and they were distributed according to the oil type. In some regions, the distributions of different oils get overlapped. This means that it may not be possible to characterize an oil using only a sole SARA composition set. In this work, we would rather use one W for each oil type (bitumen/heavy-oil/medium-oil/light-oil). For the set of 341 crude oil compositions studied in this work,[7−116] Figures 1−4 reveal that there are "empty" regions where some SARA compositions are simply impossible. For instance, neither a light-oil with values of saturates fraction around 5 wt %, and with aromatic fractions of 40 wt % nor an asphaltene fraction around 40% and with saturate fraction of 50% either can occur.

Table 2. Input Data to the Calculation Example[a]

	light-end composition		bubblepoint envelope	
type of crude oil	compound	mole fraction (%)	T (K)	P^{bp} (MPa)
light	H_2S	5.39	348.15	14.48
	N_2	0.91	363.15	16.55
	CO_2	1.57	393.15	17.93
			413.15	19.31

[a]Data were taken from ref 3 (Well_3).

Table 3. Values of the Regressed Factors Employed in Equations 1 and 2

B^{bp} (K^{-1} MPa)	0.057778821
$f^{bp}_{H_2S}$ (K MPa^{-1})	−1.0265795
$f^{bp}_{N_2}$ (K MPa^{-1})	−2.708388597
$f^{bp}_{CO_2}$ (K MPa^{-1})	8.593888235
f^{bp}_{sat} (K MPa^{-1})	0.308387207
f^{bp}_{arom} (K MPa^{-1})	−0.143981998
f^{bp}_{res} (K MPa^{-1})	−0.998941672
f^{bp}_{asp}(K MPa^{-1})	−2.98440823

Table 4. Most-Probable SARA Compositions for Well_3 of Reference 3

saturates	aromatics	resins	asphaltenes	frequency
47.0	38.0	12.79	2.210	10
47.0	39.0	11.36	2.640	10
48.0	32.0	19.72	0.284	10
48.0	33.0	18.29	0.715	10
49.0	31.0	19.49	0.512	10
49.0	32.0	18.06	0.943	10
49.0	33.0	16.63	1.373	10
49.0	34.0	15.20	1.804	10
49.0	35.0	13.77	2.235	10
49.0	36.0	12.33	2.665	10
49.0	37.0	10.90	3.096	10
50.0	32.0	16.40	1.601	10
50.0	33.0	14.97	2.032	10
51.0	35.0	10.45	3.552	10
52.0	30.0	15.94	2.057	10
52.0	31.0	14.51	2.488	10
52.0	32.0	13.08	2.918	10
52.0	33.0	11.65	3.349	10
52.0	34.0	10.22	3.779	10
53.0	30.0	14.28	2.715	10
53.0	31.0	12.85	3.146	10
53.0	32.0	11.42	3.577	10
54.0	30.0	12.63	3.374	10
54.0	31.0	11.20	3.804	10
55.0	30.0	10.97	4.032	10

DOI: 10.1021/acs.energyfuels.6b00614
Energy Fuels 2016, 30, 6913−6922

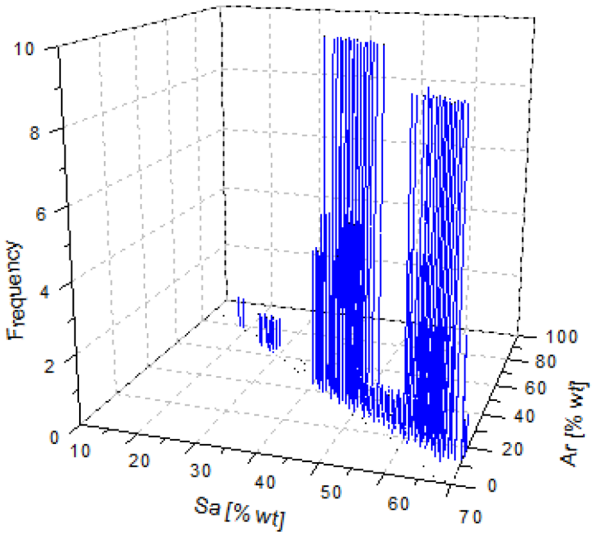

Figure 8. Histogram of absolute frequencies of t_{Sa} and t_{Ar} which fulfill with the bubblepoint pressure data of well 3.

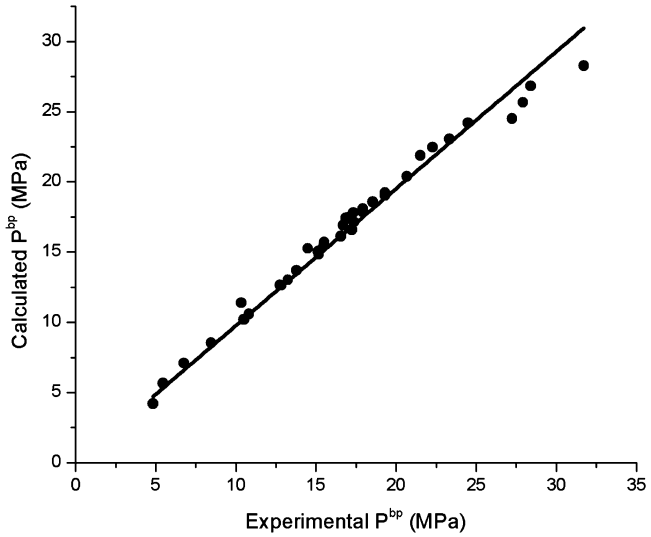

Figure 9. Correlation between bubblepoint pressures obtained from estimated SARA compositions and experimental bubblepoint pressures.

Table 5. Sample Calculation of the Error Assignation to the Different SARA Compositions with Maximum Absolute Frequency

saturates	aromatics	resins	asphaltenes	error
54.0	31.0	11.20	3.804	0.3903
46.0	36.0	17.31	0.690	0.3905
47.0	35.0	17.08	0.918	0.3906
45.0	37.0	17.54	0.462	0.3907
44.0	38.0	17.77	0.234	0.3907
51.0	34.0	11.88	3.121	0.3907
55.0	30.0	10.97	4.032	0.3908
46.0	38.0	14.45	1.551	0.3909
46.0	39.0	13.02	1.982	0.3909
48.0	34.0	16.85	1.146	0.3910

The probability density W, for an oil, was estimated by the histogram of SARA compositions taken from the data set.[7−116] As occur in all histograms in statistics, if the mesh size is big enough, it is not possible to obtain reasonably detailed trends and, if the mesh is small enough, new classes appear in the histogram, with a null value of probability, giving highly irregular and random trends. In our case, a mesh with a cell length of 10% was chosen. Other cell lengths could also be assumed.

Figure 7 shows the flow diagram of the calculations carried out in the proposed method. A step-by-step sample calculation for a test oil will now be presented. The same calculations are applicable to any other oil system.

Step 1: The type of crude oil (light, medium, or heavy), the light-end composition, and the bubblepoint data set are input as the data set to a problem. As an example (see Table 2), data of "well-3" of ref 3 were taken.

Step 2: Calculation of the $f^{bp}(C^{bp})$ term from bubble point data: This term is calculated using the following equation:

$$f^{bp}(C^{bp}) = \frac{1}{n}\sum_{i=1}^{n}(P_i^{bp} - B^{bp}T_i) \tag{16}$$

where n is the number of data points in the bubble pressure envelope. In our example (Table 2) $n = 4$. P^{bp}_i and T_i are the data of pressure and temperature of the experimental bubblepoint envelope, and B^{bp} is the constant of eq 1 whose value is shown in Table 3. In the calculation example $f^{bp}(C^{bp}) = -4.853784$.

Table 6. Experimental SARA Compositions Taken from the Reference 3 and Data Calculated Using the Method Presented in This Work

experimental data (wt %)				data calculated by the proposed method (wt %)							
				saturates and aromatics taken as independent variables				resins and asphaltenes taken as independent variables			
tSa	tAr	tRe	tAs	tSa	tAr	tRe	tAs	tSa	tAr	tRe	tAs
31.5	49.49	14.3	4.06	41	39	14.16	5.84	41.7	38.3	14	6
36.12	45.78	14.06	3.04	46	38	11.45	4.55	48	36.02	11	5
54.67	28.89	13.36	3.08	54	31	11.2	3.8	53	33.03	10	4
33.63	37.21	14.33	14.83	19	57	10.15	13.85	17.2	57.8	12	13
59.28	30.58	9.41	0.73	55	36	7.54	1.46	58	35	4	3
43.87	43.29	9.74	3.1	52	32	11.4	4.6	53.8	30.2	11	5
46.89	33.07	17.3	2.72	49	36	10.29	4.7	45.9	39.1	11	4
44.65	34.55	14.9	2.86	47	32	18.92	2.08	46	38	12	4
46.48	34.34	17.74	1.43	49	30	18.78	2.22	45	39	11	4
55.14	30.73	11.42	4.21	54	30	11.17	4.83	52.8	32.2	10	5

DOI: 10.1021/acs.energyfuels.6b00614
Energy Fuels 2016, 30, 6913−6922

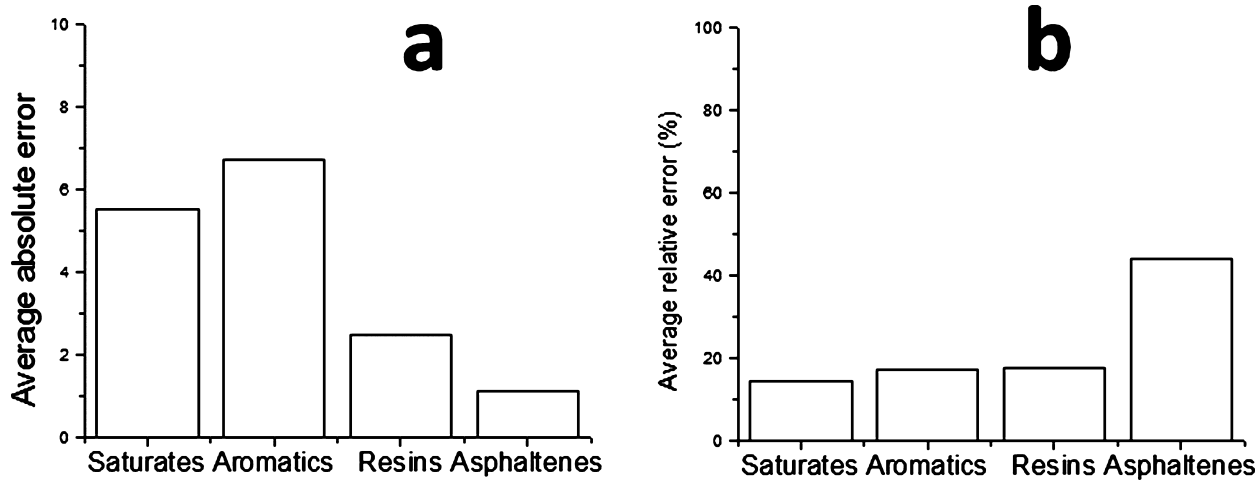

Figure 10. (a) Averaged absolute errors of the SARA compositions calculated using the method presented in this work. (b) Averaged relative errors of the SARA compositions calculated using the method presented in this work.

Step 3: Since all SARA compositions must add up to 100%, and from eq 11, two of the SARA variables can be expressed as a function of the other two, we choose t_{Sa}, t_{Ar} as independent variables in this work (see eqs 12 and 13). In this way, we only have to scan all possible values of t_{Sa}, t_{Ar}. The mesh to carry out this search can be made in the following way. Because all SARA variables must be non-negative and their addition must add up tp 100%, one independent variable (for example t_{Sa}) can vary from 0 to 100. In this way, the other variable (t_{Ar}) will vary from 0 to 100 − t_{Sa}. Figure 6a shows the mesh with these characteristics used in this work. The length cell was 10% because the histogram of SARA compositions was obtained with this length interval.

Step 4: The mesh is scanned using the central points of each cell. In this way for each pair (t_{Sa}, t_{Ar}) the values of t_{Re}, t_{As}, compatible with the bubblepoint data set, were calculated using eqs 12 and 13. Only non-negative values are accepted. Table 4 shows the several SARA compositions of the calculation example compatible with the bubblepoint data set. For each set of SARA composition, a value of probability was assigned using the histogram of SARA compositions. Table 4 shows examples of these assignations. For convenience, the absolute frequency was used as a measure of the probability. Figure 6b shows an example on how both the function buildup using the mesh, and the assignation of a probability to each cell of the mesh are made. The cells with maximum probability were stored.

Step 5: Check if there are more than one SARA compositions with maximum absolute frecuency. If only one composition fulfills this condition go to step 8. Otherwise go to step 6.

Step 6: For each of the SARA compositions with maximum absolute frequency, Table 4 shows that it is possible to find a set of SARA compositions with maximum probability and being compatible with a given bubblepoint envelope. Figure 8 shows the absolute frequency of t_{Sa} and $t_{Ar.}$ A criterion to choose a particular SARA composition is the following. From eqs 1 and 2, it is possible to calculate a bubblepoint pressure (P^{bpCALC}) for each SARA composition using the coefficients of Table 3. In this way, an error was assigned to each SARA composition as

$$\text{error} = \frac{1}{n}\sum_{i=1}^{n} |P_i^{bpEXP} - P_i^{bpCALC}| \quad (17)$$

Table 5 shows examples of the assigned errors with this procedure.

Step 7: Select the SARA composition with less error: An error was assigned to each SARA composition; the selected SARA composition will be the composition with the lowest error. For the calculation example, the results are t_{Sa} = 54%, t_{Ar} = 31%, t_{Re} = 11.2, and t_{As} = 3.8%, which is near the measured real SARA analysis (t_{Sa} = 54.67%, t_{Ar} = 28.89%, t_{Re} = 13.36, and t_{As} = 3.08%) taken from ref 3.

Step 8: The calculations conclude.

The proposed method was tested with a number of oils whose characterization parameters were taken from ref 3, and the results are shown in Table 6. . Figure 9 shows the correlation between P^{bpEXP} and P^{bpCALC} for 31 available bubblepoint pressure data points from our database. The data are very close to the straight line $y = x$, indicating a good correlation.

Figure 10a shows the average absolute errors for each SARA fraction. The average absolute error for the saturate and aromatics fractions is bigger than that for the resin and asphaltene fractions because usually t_{Sa} and t_{Ar} are bigger than t_{Re} and t_{As}. Figure 10b shows the average relative errors. It is interesting to observe that this error for the saturated, aromatic, and resin fractions is almost constant (around 16%), while that for the asphaltene fraction is higher (around 45%). This fact can be explained in terms in which the SARA compositions for aromatics, saturates, and resins are bigger than for asphaltenes (Figure 3a shows clearly that t_{As} is mainly distributed below 25%). For this reason the averaged absolute deviations are smaller for the asphaltene compositions. On the other hand, because the asphaltene SARA composition is often smaller, the relative errors are higher. Despite the availability of 341 data sets for the entire model, these are distributed to build bitumen, heavy-oil, medium-oil, and light-oil histograms, where different data sets are available. This relates with the predictive capability of the model.

In this work t_{Sa} and t_{Ar} were used as independent variables. This selection is arbitrary. A different possibility could be, for instance, to choose t_{Re} and t_{As} as independent variables. Table 6 shows the obtained results using t_{Re} and t_{As} as independent variables. The results are very similar.

DOI: 10.1021/acs.energyfuels.6b00614
Energy Fuels 2016, 30, 6913−6922

CONCLUSIONS

We have presented a method for estimating the most-probable SARA compositions in petroleum fluids using available light-end compositions and bubblepoint pressure data only. By using available SARA data of a wealth of crude oils of different origin, we have shown for the first time that not all SARA compositions for an oil are physically possible.

An advantage of the proposed method is its simplicity. It could be used with other empirical correlations[4,5] or theoretical models[115,116] as numerical closures (eqs 9–11). In a future improvement, we will enhance our database by including more experimental data.

To provide further accuracy to the proposed method, an approach could incorporate the fulfilling of more restrictions, i.e., to reproduce other measured properties of the oil in consideration. One limitation of the numerical method used is that its precision depends on the size of the meshes (the mesh of the histogram and the mesh for the maximum search). This problem can be avoided by using more sophisticated interpolation methods, i.e., methods based on splines,[6]

ASSOCIATED CONTENT

Supporting Information

The Supporting Information is available free of charge on the ACS Publications website at DOI: 10.1021/acs.energyfuels.6b00614.

SARA compositions, crude oil type, geographic region of origin, and references for all 341 crude oils (XLSX)

Special Issue Paper

Part of the special issue 16th International Conference on Petroleum Phase Behavior and Fouling.

AUTHOR INFORMATION

Corresponding Authors

*(C.L.-G.) E-mail: clira@imp.mx.

*(J.M.d.R.) E-mail: jmdelrio@imp.mx.

Notes

The authors declare no competing financial interest.

ACKNOWLEDGMENTS

D.R.-G. expresses his gratitude to CONACyT and the National University of Mexico for a graduate fellowship. We thank the authorities of the Mexican Institute of Petroleum, Project H.61038, for permission to publish this work.

REFERENCES

(1) Leontaritis, K. J. *Fuel Sci. Technol. Int.* **1996**, *14*, 13.

(2) Ramirez-Jaramillo, E.; Lira-Galeana, C.; Manero, O. *Energy Fuels* **2006**, *20*, 1184.

(3) del Rio, J.; Ramirez-Jaramillo, E.; Lira-Galeana, C. *AIChE J.* **2009**, *55*, 1814.

(4) Fahim, M. *Pet. Sci. Technol.* **2007**, *25*, 949.

(5) Fahim, M. A. *Pet. Sci. Technol.* **2007**, *25*, 1605.

(6) Viola, F.; Coe, R. L.; Owen, K.; Guenther, D. A.; Walker, W. F. *Ann. Biomed. Eng.* **2008**, *36* (12), 1942.

(7) Lesaint, C.; Vrålstad, H.; Spets, Ø.; Simon, S.; Hannisdal, A.; Lundgaard, L.; Lihnjell, D.; Sjoblom, J. *J. Dispersion Sci. Technol.* **2011**, *32*, 874.

(8) Rogel, E.; León, O.; Contreras, E.; Carbognani, L.; Torres, G.; Espidel, J.; Zambrano, A. *Energy Fuels* **2003**, *17*, 1583.

(9) Aske, N.; Kallevik, H.; Sjöblom, J. *Energy Fuels* **2001**, *15*, 1304.

(10) Castro, L. V.; Vazquez, F. *Energy Fuels* **2009**, *23*, 1603.

(11) Zhao, B.; Shaw, J. M. *Energy Fuels* **2007**, *21*, 2795.

(12) Wang, J.; Buckley, J. S. *Energy Fuels* **2003**, *17*, 1445.

(13) Kök, M. V.; Karacan, O.; Pamir, R. *Energy Fuels* **1998**, *12*, 580.

(14) Al-Saffar, H. B.; Hasanin, H.; Price, D.; Hughes, R. *Energy Fuels* **2001**, *15*, 182.

(15) Cinar, M.; Castanier, L. M.; Kovscek, A. R. *Energy Fuels* **2011**, *25*, 4438.

(16) Peramanu, S.; Singh, C.; Agrawala, M.; Yarranton, H. W. *Energy Fuels* **2001**, *15*, 910.

(17) Bisht, H.; Reddy, M.; Malvanker, M.; Patil, R. C.; Gupta, A.; Hazarika, B.; Das, A. k. *Energy Fuels* **2013**, *27*, 3006.

(18) Islas-Flores, C. A.; Buenrostro-Gonzalez, E.; Lira-Galeana, C. *Energy Fuels* **2005**, *19*, 2080.

(19) Hauser, A.; AlHumaidan, F.; Al-Rabiah, H.; Halabi, M. A. *Energy Fuels* **2014**, *28*, 4321.

(20) Riveros, L.; Jaimes, B.; Ranaudo, M. A.; Castillo, J.; Chirinos, J. *Energy Fuels* **2006**, *20*, 227.

(21) Carbognani, L.; Gonzalez, M. F.; Pereira-Almao, P. *Energy Fuels* **2007**, *21*, 1631.

(22) Zhao, B.; Becerra, M.; Shaw, J. M. *Energy Fuels* **2009**, *23*, 4431.

(23) Tharanivasan, A. K.; Yarranton, H. W.; Taylor, S. D. *Energy Fuels* **2011**, *25*, 528.

(24) Liu, Y.; Fan, H. *Energy Fuels* **2002**, *16*, 842.

(25) Akbarzadeh, k.; Dhillon, A.; Svrcek, W. Y.; Yarranton, H. W. *Energy Fuels* **2004**, *18*, 1434.

(26) Niu, B.; Ren, S.; Liu, Y.; Wang, D.; Tang, L.; Chen, B. *Energy Fuels* **2011**, *25*, 4299.

(27) Barcenas, M.; Orea, P.; Buenrostro-Gonzalez, E.; Zamudio-Rivera, L. S.; Duda, Y. *Energy Fuels* **2008**, *22*, 1917.

(28) Juyal, P.; McKenna, A. M.; Yen, A.; Rodgers, R. P.; Reddy, C. P.; Nelson, R. K.; Andrews, A. B.; Atolia, E.; Allenson, S. J.; Mullins, O. C.; Marshall, A. G. *Energy Fuels* **2011**, *25*, 172.

(29) Deng, W.; Luo, H.; Gao, J.; Que, G. *Energy Fuels* **2011**, *25*, 5360.

(30) Shi, T.-P.; Xu, Z.-M.; Cheng, M.; Hu, Y.-X.; Wang, R.-A. *Energy Fuels* **1999**, *13*, 871.

(31) Satya, S.; Roehner, R. M.; Deo, M. D.; Hanson, F. V. *Energy Fuels* **2007**, *21*, 998.

(32) Hasan, MD. A.; Fulem, M.; Bazyleva, A.; Shaw, J. M. *Energy Fuels* **2009**, *23*, 5012.

(33) Seiedi, O.; Rahbar, M.; Nabipour, M.; Emadi, M. A.; Ghatee, M. H.; Ayatollahi, S. *Energy Fuels* **2011**, *25*, 183.

(34) de Oliveira, M. C. K.; Teixeira, A.; Vieira, L. C.; de Carvalho, R. M.; de Carvalho, A. B. M.; do Couto, B. C. *Energy Fuels* **2012**, *26*, 2688.

(35) Alvarez, G.; Poteau, S.; Argillier, J.-F.; Langevin, D.; Salager, J.-L. *Energy Fuels* **2009**, *23*, 294.

(36) Flego, C.; Zannoni, C. *Energy Fuels* **2013**, *27*, 46.

(37) Meyer, V.; Pilliez, J.; Habas, J.-P.; Montel, F.; Creux, P. *Energy Fuels* **2008**, *22*, 3154.

(38) Mortazavi-Manesh, S.; Shaw, J. M. *Energy Fuels* **2014**, *28*, 972.

(39) Ghatee, M. H.; Hemmateenejad, B.; Sedghamiz, T.; Khosousi, T.; Ayatollahi, S.; Seiedi, O.; Sayyad Amin, J. *Energy Fuels* **2012**, *26*, 5663.

(40) Solaimany-Nazar, A. R.; Rahimi, H. *Energy Fuels* **2009**, *23*, 967.

(41) Soto-Castruita, E.; Ramirez-Gonzalez, P. V.; Martinez-Cortes, U.; Quiñones-Cisneros, S. E. *Energy Fuels* **2015**, *29*, 2883 (15th International Conference on Petroleum Phase Behavior and Fouling).

(42) Rezaei, N.; Mohammadzadeh, O.; Chatzis, I. *Energy Fuels* **2010**, *24*, 5934.

(43) Gawel, B.; Eftekhardadkhah, M.; Øye. *Energy Fuels* **2014**, *28*, 997.

(44) Jarne, C.; Cebolla, V. L.; Membrado, L.; Le Mapihan, K.; Giusti, P. *Energy Fuels* **2011**, *25*, 4586.

(45) de Oliveira, L. P.; Vazquez, A. T.; Verstraete, J. J.; Kolb, M. *Energy Fuels* **2013**, *27*, 3622.

(46) Gonzalez, D. L.; Ting, P. D.; Hirasaki, G. J.; Chapman, W. G. *Energy Fuels* **2005**, *19*, 1230.

(47) Carbognani, L.; Buenrostro-Gonzalez, E. *Energy Fuels* **2006**, *20*, 1137.

DOI: 10.1021/acs.energyfuels.6b00614
Energy Fuels 2016, 30, 6913–6922

(48) Fan, M.; Sun, X.; Xu, Z.; Zhao, S.; Xu, C.; Chung, K. H. *Energy Fuels* **2011**, *25*, 3060.
(49) Fan, T.; Wang, J.; Buckley, J. S. Evaluating Crude Oils by SARA Analysis. *SPE/DOE Improved Oil Recovery Symposium*, SPE-75228-MS, Tulsa, OK, USA; Society of Petroleum Engineers: Richardson, TX, USA, 2002; DOI: 10.2118/75228-MS.
(50) Xia, T. X.; Greaves, M. Downhole Upgrading Athabasca Tar Sand Bitumen Using THAI-SARA Analysis. *International Thermal Operations and Heavy Oil Symposium*, SPE-69693-MS, Porlamar, Margarita Island, Venezuela; Society of Petroleum Engineers: Richardson, TX, USA, 2001; DOI: 10.2118/69693-MS.
(51) Kok, M. V.; Karacan, C. O. Behavior and Effect of SARA Fractions of Oil During Combustion. *SPE Reservoir Evaluation & Engineering*, SPE-66021-PA; 1997 SPE International Thermal Operations & Heavy Oil Symposium, Bakersfield, CA, USA; Society of Petroleum Engineers: Richardson, TX, USA, 2000; p 380, DOI: 10.2118/66021-PA.
(52) Juyal, p.; McKenna, A. M.; Fan, T.; Cao, T.; Rueda-Velasquez, R. I.; Fitzsimmons, J. E.; Yen, A.; Rodgers, R. P.; Wang, J.; Buckley, J. S.; Gray, M. S.; Allenson, S. J.; Creek, J. *Energy Fuels* **2013**, *27*, 1899.
(53) Daridon, J. L.; Cassiede, M.; Nasri, D.; Pauly, J.; Carrier, H. *Energy Fuels* **2013**, *27*, 4639.
(54) Juyal, P.; Yen, A. T.; Rodgers, R. P.; Allenson, S.; Wang, J.; Creek, J. *Energy Fuels* **2010**, *24*, 2320.
(55) Verdier, S.; Carrier, H.; Andersen, S. I.; Daridon, J.-L. *Energy Fuels* **2006**, *20*, 1584.
(56) Hendraningrat, L.; Torsæter, O. *Energy Fuels* **2014**, *28*, 6228.
(57) Poteau, S.; Argillier, J.-F.; Langevin, D.; Pincet, F.; Perez, E. *Energy Fuels* **2005**, *19*, 1337.
(58) Montel, V.; Lazzeri, V.; Brocart, B.; Zhou, H. *Energy Fuels* **2008**, *22*, 3970.
(59) Varet, G.; Montel, F.; Nasri, D.; Daridon, J.-L. *Energy Fuels* **2013**, *27*, 2528.
(60) Abivin, P.; Taylor, S. D.; Freed, D. *Energy Fuels* **2012**, *26*, 3448.
(61) Kord, S.; Miri, R.; Ayatollahi, S.; Escrochi, M. *Energy Fuels* **2012**, *26*, 6186.
(62) Paso, K.; Silset, A.; Sørland, G.; Gonçalves, M. d. A. L.; Sjöblom, J. *Energy Fuels* **2009**, *23*, 471.
(63) Mendoza de la Cruz, J. L.; Argüelles-Vivas, F. J.; Matías-Pérez, V.; Durán-Valencia, C. d. l. A.; López-Ramirez, S. *Energy Fuels* **2009**, *23*, 5611.
(64) Ocanto, O.; Marcano, F.; Castillo, J.; Fernandez, A.; Caetano, M.; Chirinos, J.; Ranaudo, M. A. *Energy Fuels* **2009**, *23*, 3039.
(65) Sakthivel, S.; Velusamy, S.; Gardas, R. L.; Sangwai, J. S. *Energy Fuels* **2014**, *28*, 6151.
(66) Juyal, P.; Ho, V.; Yen, A.; Allenson, S. J. *Energy Fuels* **2012**, *26*, 2631.
(67) Kakati, H.; Kar, S.; Mandal, A.; Laik, S. *Energy Fuels* **2014**, *28*, 4440.
(68) Kariznovi, M.; Nourozieh, H.; Abedi, J. *Energy Fuels* **2014**, *28*, 7418.
(69) Zielinski, L.; Hürlimann. *Energy Fuels* **2011**, *25*, 5090.
(70) Michon, L. C.; Netzel, D. A.; Turner, T. F.; Martin, D.; Planche, J.-P. *Energy Fuels* **1999**, *13*, 602.
(71) Wang, X.; Xu, Z.; Zhao, S.; Xu, C.; Chung, K. H. *Energy Fuels* **2009**, *23*, 386.
(72) Nourozieh, H.; Kariznovi, M.; Abedi, J. *Energy Fuels* **2014**, *28*, 2874.
(73) Jafari Behbahani, T.; Ghotbi, C.; Taghikhani, V.; Shahrabadi, A. *Energy Fuels* **2012**, *26*, 5080.
(74) Acevedo, S.; Rodriguez, P.; Labrador, H. *Energy Fuels* **2004**, *18*, 1757.
(75) Wang, H.; Wu, Y.; He, L.; Liu, Z. *Energy Fuels* **2012**, *26*, 6518.
(76) Xu, H.; Pu, C.; Wu, F. *Energy Fuels* **2012**, *26*, 5655.
(77) Gonçalves, J. L.; Bombard, A. J. F.; Soares, D. A. W.; Carvalho, R. D. M.; Nascimento, A.; Silva, M. R.; Alcântara, G. B.; Pelegrini, F.; Vieira, E. D.; Pirota, K. R.; Bueno, M. I. M. S.; Lucas, G. M. S.; Rocha, N. O. *Energy Fuels* **2011**, *25*, 3537.
(78) Wang, H.-L.; Wang, G.; Zhang, D. C.; Xu, C.-M.; Gao, J.-S. *Energy Fuels* **2012**, *26*, 4177.
(79) Yasar, M.; Trauth, D. M.; Klein, M. T. *Energy Fuels* **2001**, *15*, 504.
(80) Zhang, T.; Zhang, L.; Zhou, Y.; Wei, Q.; Chung, K. H.; Zhao, S.; Xu, C.; Shi, Q. *Energy Fuels* **2013**, *27*, 2952.
(81) Gonzalez, D. L.; Vargas, F. M.; Hirasaki, G. J.; Chapman, W. G. *Energy Fuels* **2008**, *22*, 757.
(82) Chang, J.; Fujimoto, K.; Tsubaki, N. *Energy Fuels* **2003**, *17*, 457.
(83) Kurup, A. S.; Vargas, F. M.; Wang, J.; Buckley, J.; Creek, J. L.; Subramani, H. J.; Chapman, W. G. *Energy Fuels* **2011**, *25*, 4506.
(84) Durand, E.; Clemancey, M.; Lancelin, J.-M.; Verstraete, J.; Espinat, D.; Quoineaud, A.-A. *Energy Fuels* **2010**, *24*, 1051.
(85) Maqbool, T.; Raha, S.; Hoepfner, M. P.; Fogler, H. S. *Energy Fuels* **2011**, *25*, 1585.
(86) Ibrahim, H. H.; Idem, R. O. *Energy Fuels* **2004**, *18*, 743.
(87) Aguiar, J. I. S.; Garreto, M. S. E.; Gonzalez, G.; Lucas, E. F.; Mansur, C. R. E. *Energy Fuels* **2014**, *28*, 409.
(88) Cardoso, F. M. R.; Carrier, H.; Daridon, J.-L.; Pauly, J.; Rosa, P. T. V. *Energy Fuels* **2014**, *28*, 6780.
(89) Tichelkamp, T.; Vu, Y.; Nourani, M.; Øye, G. *Energy Fuels* **2014**, *28*, 2408.
(90) Kekäläinen, T.; Pakarinen, J. M. H.; Wickström, K.; Lobodin, V. V.; McKenna, A. M.; Jänis, J. *Energy Fuels* **2013**, *27*, 2002.
(91) Kuppe, G. J. M.; Mehta, S. A.; Moore, R. G.; Ursenbach, M. G.; Zalewski, E. *J. Can. Pet. Technol.* **2008**, *47*, 38.
(92) Kok, M. V.; Karacan, C. O. Behavior and Effect of SARA Fractions of Oil During Combustion. *1997 SPE International Thermal Operations & Heavy Oil Symposium*, SPE-37559-MS, Bakersfield, CA, USA; Society of Petroleum Engineers: Richardson, TX, USA, 1997; DOI: 10.2118/37559-MS.
(93) Verkoczy. *J. Can. Pet. Technol.* **1993**, *32* (7), 25.
(94) Akin, S.; Kok, M. V.; Bagci, S.; Karacan, O. Oxidation of Heavy Oil and Their SARA Fractions: Its Role in Modeling In-Situ Combustion. *SPE Annual Technical Conference and Exhibition*, SPE-63230-MS, Dallas, TX, USA; Society of Petroleum Engineers: Richardson, TX, USA, 2000; DOI: 10.2118/63230-MS.
(95) Fuhr, B. J.; Holloway, L. R.; Reichert, C. *J. Can. Pet. Technol.* **1986**, *25*, 01.
(96) Lamoureux-Var, V.; Lorant, F. H_2S Artificial Formation as a Result of Steam Injection for EOR: A Compositional Kinetic Approach. *International Thermal Operations and Heavy Oil Symposium*, Calgary, Alberta, Canada, SPE/PS-CIM/CHOA 97810, PS2005-375; Society of Petroleum Engineers: Richardson, TX, USA, 2005; DOI: 10.2118/97810-MS.
(97) Yen, A.; Yin, Y. R.; Asomaning, S. Evaluating Asphaltene Inhibitors: Laboratory Tests and Field Studies. *International Symposium on Oilfield Chemistry*, Houston, TX, USA, SPE-65376-MS; Society of Petroleum Engineers: Richardson, TX, USA, 2001; DOI: 10.2118/65376-MS.
(98) Jha, N. K.; Jamal, M. S.; Singh, D.; Prasad, U. S. Characterization of Crude Oil of Upper Assam Field for Flow Assurance. *Saudi Arania Section Annual Technical Symposium and Exhibition*, Al-Khobar, Saudi Arabia, SPE-172226-MS; Society of Petroleum Engineers: Richardson, TX, USA, 2014; DOI: 10.2118/172226-MS.
(99) Ferreira, S. R.; Oliveira, A. P.; Pucciarelli, N.; Tooge, C. A. B.; Souza, R. Green Products for Reducing the Viscosity of Heavy Oils. *SPE Heavy and Extra Heavy Oil Conference*, Medellin, Colombia, SPE-171082-MS; Society of Petroleum Engineers: Richardson, TX, USA, 2014; DOI: 10.2118/171082-MS.
(100) Poindexter, M. K.; Chuai, S.; Marble, R. A.; Marsh, S. C. The Key To Predicting Emulsion Stability: Solid Content. *SPE International Symposium on Oilfield Chemistry*, The Woodlands, TX, USA, SPE-93008-MS; Society of Petroleum Engineers: Richardson, TX, USA, 2005; DOI: 10.2118/93008-MS.
(101) Arciniegas, L.; Babadagli, T. Optimal Application Conditions of Solvent Injection into Oilsands to Minimize the Effect of Asphaltene Deposition: An Experimental Investigation. *SPE Heavy Oil Conference—Canada*, Calgary, Alberta, Canada, SPE-165531-MS;

DOI: 10.1021/acs.energyfuels.6b00614
Energy Fuels 2016, 30, 6913−6922

Society of Petroleum Engineers: Richardson, TX, USA, 2013; DOI: 10.2118/165531-MS.
(102) Syed, F. I.; Ghedan, S. G.; Al-Hage, A.; Tariq, S. M. Formation Flow Impairment in Carbonate Reservoirs Due to Asphaltene Precipitation and Deposition during Hydrocarbon Gas Flooding. *Abu Dhabi International Petroleum Exhibition & Conference*, Abu Dhabi, UAE, SPE-160253-MS; Society of Petroleum Engineers: Richardson, TX, USA, 2012; DOI: 10.2118/160253-MS.
(103) Greaves, M.; Xia, T. X. Underground Upgrading of Heavy Oil Using THAI-'Toe-to-Heel Air Injection'. *SPE International Thermal Operations and Heavy Oil Symposium*, Calgary, Alberta, Canada, SPE/PS-CIM/CHOA 97728, PS2005-323; Society of Petroleum Engineers: Richardson, TX, USA, 2005; DOI: 10.2118/97728-MS.
(104) Mahzari, P.; Sohrabi, M. Crude Oil/Brine Interactions and Spontaneous Formation of Micro-Dispersions in Low Salinity Water Injection. *SPE Improved Oil Recovery Symposium*, Tulsa, OK, USA, SPE-169081-MS; Society of Petroleum Engineers: Richardson, TX, USA, 2014; DOI: 10.2118/169081-MS.
(105) Mendez, A.; Duplat, S.; Hernandez, S.; Vera, J. On the Mechanism of Corrosion Inhibition by Crude Oils. *Corrosion 2001*, NACE International Conference and Exhibition, Houston, TX, USA, Document ID NACE-01030 (Paper No. 01044); NACE International: Houston, TX, USA, 2001.
(106) Kurup, A.; Valori, A.; Bachman, H. N.; Korb, J.-P.; Hürlimann, M.; Zielinski, L. Frequency Dependent Magnetic Resonance of Heavy Crude Oils: Methods and Applications. *Saudi Arabia Section Annual Technical Symposium and Exhibition*, Al-Khobar, Saudi Arabia, SPE-168070-MS; Society of Petroleum Engineers: Richardson, TX, USA, 2013; DOI: 10.2118/168070-MS.
(107) Akbarzadeh, K.; Sabbagh, O.; Beck, J.; Svrcek, W. Y.; Yarranton, H. W. Asphaltene Precipitation From Bitumen Diluted With n-Alkanes. *Canadian International Petroleum Conference*, Calgary, Alberta, Canada, PETSOC-2004-026-EA; Petroleum Society of Canada: Calgary, Canada, 2004; DOI: 10.2118/2004-026-EA.
(108) Hamid, K. Determination of the Zone of Maximum Probability of Asphaltenes Precipitation Utilising Experimental Data in an Iranian Carbonate Reservoir. *SPE Asia Pacific Oil & Gas Conference and Exhibition*, Adelaide, Australia, SPE-100899-MS; Society of Petroleum Engineers: Richardson, TX, USA, 2006; DOI: 10.2118/100899-MS.
(109) Garcia-James, C. J.; Pino, F.; Marin, T.; Maharaj, U. Influence of Resin/Asphaltene Ration on Paraffin Wax Deposition in Crude Oils from Barrackpore Oilfield in Trinidad. *SPETT 2012 Energy Conference and Exhibition*, Port-of-Spain, Trinidad, SPE-158106-MS; Society of Petroleum Engineers: Richardson, TX, USA, 2012; DOI: 10.2118/158106-MS.
(110) Gonzalez, D. L.; Mahmoodaghdam, E.; Lim, F. H.; Joshi, N. B. Effects of Gas Additions to Deepwater Gulf of Mexico Reservoir Oil: Experimental inestigation of Asphaltene Precipitation and Deposition. *SPE Annual Technical Conference and Exhibition*, San Antonio, TX, USA, SPE-159098-MS; Society of Petroleum Engineers: Richardson, TX, USA, 2012; DOI: 10.2118/159098-MS.
(111) Zhong, L. G.; Liu, Y. J.; Fan, H. F.; Jiang, S. J. Liaohe Extra-Heavy Crude Oil Underground Aquathermolytic Treatments Using Catalyst and Hydrogen Donors under Steam Injection Conditions. *SPE International improved Oil Recovery Conference in Asia Pacific*, Kuala Lumpur, Malasya, SPE-84863-MS; Society of Petroleum Engineers: Richardson, TX, USA, 2003; DOI: 10.2118/84863-MS.
(112) Jiang, S.; Liu, X.; Liu, Y.; Zhong, L. In Situ Upgrading Heavy Oil by Aquathermolytic Treatment Under Steam Injection Conditions. *SPE International Symposium on Oilfield Chemistry*, The Woodlands, TX, USA, SPE-91973-MS; SPE Production & Facilities: Richardson, TX, USA, 2005; DOI: 10.2118/91973-MS.
(113) Rogel, E.; Leon, O.; Espidel, Y.; Gonzalez, Y. Asphaltene Stability in Crude Oils. *Latin America and Caribbean Petroleum Engineering Conference*, Caracas, Venezuela, SPE-72050-PA; Society of Petroleum Engineers: Richardson, TX, USA, 2001; DOI: 10.2118/72050-PA.
(114) Li, Z.; Firoozabadi, A. *Energy Fuels* **2010**, *24*, 2956−2963.
(115) Arya, A.; von Solms, N.; Kontogeorgis, G. M. *Fluid Phase Equilib.* **2015**, *400*, 8−19.
(116) Kamari, A.; Safiri, A.; Mohammadi, A. H. *J. Dispersion Sci. Technol.* **2015**, *36*, 301−309.

DOI: 10.1021/acs.energyfuels.6b00614
Energy Fuels 2016, 30, 6913−6922